AIChE

Modeling Transdermal Permeation. Part 2. Predicting the Dermatopharmacokinetics of Percutaneous Solute

Guoping Lian
Unilever R&D Colworth, Sharnbrook, Bedford MK44 1LQ, U.K.

Longjian Chen
College of Engineering, China Agricultural University, Beijing 100083, People's Republic of China

Paul D. A. Pudney and Mickaël Mélot
Unilever R&D Colworth, Sharnbrook, Bedford MK44 1LQ, U.K.

Lujia Han
College of Engineering, China Agricultural University, Beijing 100083, People's Republic of China

DOI 10.1002/aic.12146
Published online March 10, 2010 in Wiley Online Library (wileyonlinelibrary.com).

The prediction of percutaneous absorption and bioavailability in vivo*, using the recently reported "bricks-and-mortar" model is discussed. Two sets of* in vivo *data have been simulated: the tape-striping data of 4-cyanophenol and Raman spectrometry data of transretinol. The predicted transdermal permeation using theoretically derived properties agreed well with the experimental data. The prediction shows that about 2/3 of the 4-cynophenol in the SC partitioned into the corneocytes, indicating diffusion of moderately hydrophobic solutes across the corneocytes is also important. Only for highly hydrophobic solute like transretinol, diffusion across the corneocytes is negligibly small. The study demonstrates that with the mechanism-based computer model, many dermatopharmacokinetic parameters can be derived, providing much insight into how vehicle formulation and topical administration affects the absorption and distribution of solute in the SC, as well as its bioavailability in epidermis/dermis.* © 2010 American Institute of Chemical Engineers *AIChE J,* 56: 2551–2560, 2010
Keywords: dermatopharmacokinetics, percutaneous absorption, raman spectroscopy, stratum corneum, transdermal delivery

Introduction

Predicting the dermatopharmacokinetics of percutaneous permeation and absorption of topically applied solutes *in vivo* is of importance to the delivery of therapeutic drugs,[1–4] formulation design of cosmetic products[5] and risk assessment of hazardous chemical exposure.[6,7] Modeling transdermal solute permeation and water loss is also relevant to the diagnosis of atopic dermatitis which affects 15–20% children in developed countries.[5,8] Studies on transdermal permeation and absorption of solutes can be traced back to the 1960s.[9,10] Since then, the subject has attracted continued interest for several decades including both measurement and modeling.[11–24]

A main challenge in transdermal permeation is to determine how vehicle formulation, dosage and topical application regimes affect the distribution of solute in different

Correspondence concerning this article should be addressed to L. Chen at clj1020@googlemail.com.

layers and domains of the skin and the delivery to targeted areas.[25,26] Most studies on percutaneous permeation and absorption involve experimental methods that are *ex vivo* and/or invasive. *In vivo* measurement of transdermal permeation and absorption is very difficult and limited. Several studies have been reported using tape striping method to investigate solute distribution and absorption in the stratum corneum (SC).[27–29] Solute concentrations in different layers of the removed SC materials are analyzed by various analytical methods. Noninvasive optical microscopic techniques are used to visualize the skin morphology including the cellular structure in the epidermis.[30] Recently, progresses have been made in using confocal Raman spectrometry as a noninvasive *in vivo* method to measure the molecular composition of the skin and concentration gradients in the skin.[31] The technique has been used for noninvasive determination of molecular concentration profile of skin components such as natural moisturizing factors, lipids and hydration levels.[32,33]

The dermatopharmacokinetics of percutaneous permeation and absorption of a topically applied solute *in vivo* is a complex dynamic process influenced by many interacting factors. The aforementioned *in vivo* techniques are limited to the top SC layers of less than 20 μm, and further information of solute bioavailability in the epidermis and dermis of the skin is not directly available.[34–37] Information about the distribution and storage of solute in the SC is also averaged and not resolved into the cellular resolution between the lipid matrix and corneocytes. In order to understand how vehicle formulation and application regimes affect percutaneous solute absorption and bioavailability, it is necessary to have reliable models capable of predicting experimental data and providing solute permeation, partition and storage in different layers and phases of the heterogeneous skin. Generally, there have been limited models capable of predicting transdermal solute permeation and absorption *in vivo*. Simple diffusion models have been frequently applied, but the approach disregarded the heterogeneous structure of the SC, and are mostly applied to derive the overall diffusion and partition properties of the SC via parameter fitting to experimental data.[29] Herkenne et al.[38] presented a simple diffusion model of *in vivo* transdermal permeation and used it to fit tape-striping data to derive dermatopharmacokinetic parameters including the overall SC-vehicle partition coefficient and SC membrane diffusion coefficient. Compartmental models have been also reported,[39,40] such models remained to be theoretical and applications to *in vivo* predictions have not been reported.

We recently presented a mechanistic model for predicting transdermal permeation using theoretically estimated model parameters that are related to the structural and compositional properties of the skin.[41] The model has been applied to predict skin permeability of a large data set and it is shown that the prediction is significantly improved by including the transcelluar pathway which contribute to more than 95% of transdermal permeation of highly hydrophilic solutes.[42] In this study, the model is further applied to predict transdermal permeation and absorption of topically administered solutes *in vivo*. We first discuss the validation of the model against two sets of experimental data published elsewhere: the *in vivo* tape striping data of 4-cyanophenol[29] and confocal Ramon spectroscopic data of transretinol.[36] The predicted solute distribution in the SC agreed well with the *in vivo* data. From the computer simulation, the distribution 4-cyanophenol and transretinol in the lipid phase and corneocytes of the SC is also predicted, further elucidating the dependence of transdermal absorption on the physicochemical properties of the solute and the heterogeneous structure of the skin. In addition, the rate (flux) of solute permeation across the SC into the epidermis and dermis has been quantified. The overall aim is to demonstrate how the mechanism-based computer models can be used to predict *in vivo* experimental data and provide key bioavailability metrics of transdermal delivery that are not available directly from current *in vivo* measurement techniques.

Methods and Materials

Experimental

Tape Striping. The published *in vivo* tape striping data of 4-cyanophenol presented by Stinchcomb et al.[29] are simulated. The tape stripping experiment involved topical application of 1.4 mL of saturated aqueous solution of 4-cyanophenol to a 20 cm^2 area of skin in the ventral forearm of 25–30 years old healthy volunteers. The application periods were 1, 5 and 15 min, respectively. At the end of each application period, the excessive solution on the skin surface was wiped using water-dampened cotton, and the skin surface was gently dried. The SC at the treated site then was progressively removed by repeated adhesive tape-stripping (20 tape strips were removed). Removed mass of each tape strip was weighed. The concentration profile of 4-cyanophenol across the SC was determined using attenuated-total-reflectance Fourier-transform-infrared spectroscopy. More details of the experiment can be found in the original article.[29]

Confocal Raman. Confocal Raman spectrometry is a relatively new method used for *in vivo* measurement of the chemical composition of skin. Pudney et al.[36] showed that the technique can be adapted to measure transdermal permeation of transretinol from topically applied solutions. Their published data are also modeled. The measurements were performed on the 3510 skin composition analyzer (model 3510 SCA, River Diagnostics, Rotterdam, The Netherlands). The instrument is CE (Conformity European) marked and classified as a 2M laser device. The instrument is optimized for rapid *in vivo* measurements on the human skin and offers an axial spatial resolution of 5 μm. It comprises a high-performance dispersive spectrometer with 671 nm and 785 nm laser excitation and a confocal measurement stage. The spectrometer allows for measurements in the high-wave number region (2,400–4,000 cm^{-1}), and the finger print region (400–2,400 cm^{-1}) of the Raman spectrum. The spectral resolution is 4 cm^{-1} throughout the entire spectral range.

For the measurements, the arm of the volunteer is placed on a fused silica window mounted in the measurement stage. Laser light is focused in the skin with a microscope objective located under the window. An internal video camera allows for inspection of the skin surface and the selection of the measurement spot. The skin is in good optical contact to the measurement window, and the space between the measurement window and the microscope objective was filled with immersion oil. This way, refractive index mismatch (resulting in degraded spatial resolution and poor definition

of the position of the laser focus) is minimized.[43] The location of the laser focus relative to the skin surface can be accurately varied by changing the focusing depth automatically. Raman spectra are recorded from the skin surface down to the viable epidermis in 2 μm steps. Detailed Raman depth profiles were acquired across the stratum corneum and into the viable epidermis. In order to overcome the lateral variation in skin composition, six profiles per measurement area are typically averaged. All Raman spectra are calibrated and corrected for instrument response using built-in instrument control software of the model 3510 SCA (River Diagnostics).

Experiments were performed twice on the volar forearms of two male volunteers of age 30 and 45 years. Prior to treatments untreated part of the forearm were measured on each volunteer as the baseline. For each experiment, a test area of 4 cm $\times$ 4 cm was marked and treated with 70 μL of the solution being investigated. Solutions applied on the skin were spread gently using the tip of the micropipette, without rubbing. Measurements were started 10 min after the application of solution on the skin. No washing and no dabbing of the remaining solutions were done prior to measurements and no particular dietary restrictions were followed.

Depth profiles were collected over an hour period from different locations within the treated (or untreated) area. For each spectrum in a given profile, the exposure time was either 5 or 10 s (fingerprint spectra using the 785 nm laser) with three accumulations, and 1 s with one accumulation (high-wave number spectra using the 671 nm laser). The Raman spectra were of excellent signal-to-noise ratio, some typical spectra are shown in Figure 1. No post acquisition treatment (e.g., spectral smoothing) was carried out on the spectra. Six depth profiles were collected within each hour time period (as was done for the untreated skin) and averaged. The spectra from within the second hour after treatment at a depth of 4 microns below the skin surface are shown in Figure 1 to illustrate the typical type of variation between spectra due to biological variation. The time points of when these spectra were taken are also given in the figure. Similar numbers of depth profiles were collected every hour up to six hours after treatment. All fingerprint spectra collected through the skin were fitted using a multilinear regression model based on the spectra of the main components of the skin, as described previously.[34,35] In this case, the spectra of *trans*-retinol and PG were added. In order to prevent an occlusion effect (i.e., an increase in hydration of the skin), the arm was lifted after three or four measurements for 10 min and repositioned back onto the device to complete the series. Further details can be found in Pudney et al.[36] and Mélot et al.[35]

Computer simulation

To use our model to simulate the dermatopharmacokinetics of solute absorption and permeation under the above *in vivo* experimental condition, the epidermis and dermis beneath the SC is regarded as an infinite sink of zero concentration. All the *in vivo* data to-date[28,29,36,38] showed that the concentration of active molecules at the skin depth greater than 15 microns, is orders of magnitude lower than that in the top 0–10 μm of the SC. Thus, as far as transdermal permeation and absorption are concerned, it is reasonable to assume the dermis and epidermis beneath the SC as an infinite sink of zero concentration.

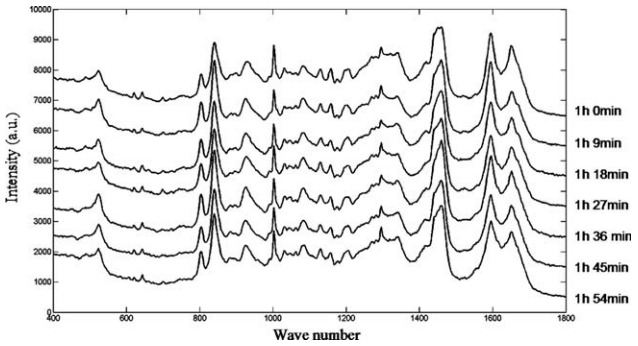

Figure 1. *In vivo* Raman spectra of skin treated with 70:30 (v/v) ethanol/propylene glycol containing 0.3% retinol at 4 microns below the surface at different positions on the skin.

The spectra were taken between one and two hours after the treatment.

The vehicle is modeled as either an infinite source with a constant concentration or a finite volume of known thickness and initial concentration depending on the condition of the topical administration. If the solute concentration in the vehicle is oversaturated and remained oversaturated during the period of experiment, the vehicle is treated as an infinite source with the constant concentration set at the saturation. Otherwise, the vehicle is modeled as a finite volume with a preset initial concentration and thickness. In this case, the concentration of the molecule in the vehicle varies with time according to the mass-balance equation. Two parameters are used to characterize the properties of the vehicle in the simulation, its diffusion coefficient and vehicle-water partition coefficient of the solute. Both can be estimated from the physical chemical properties of the solute, as well as the vehicle formulation.

The structural parameters of the ''bricks and mortar'' (Figure2) are kept to be the same as in Part 1 of this article,[42] where more details of the SC structure and composition including the calculation of the partition and diffusion properties can be found. From the computer simulation, the flux of the solute delivered to the sink (epidermis and dermis) can be obtained, from which the accumulative amount is obtained. This is often referred as the area under the curve (AUC), and is obtained by integrating the flux according to the following equation

$$M_d = \int_0^t A q_d dt \tag{1}$$

where A is the area of topical application, q_d is the predicted flux of the active molecule delivered from the SC to the sink.

The mass-balance equation of a topically applied solute has the following components

$$M_0 = M_d(t) + M_{sc}(t) + M_s(t) \tag{2}$$

where M_0 is the initial dose, $M_{sc}(t)$ is the amount of solute accumulated in the SC, and $M_s(t)$ is the amount lost due to removal and degradation.

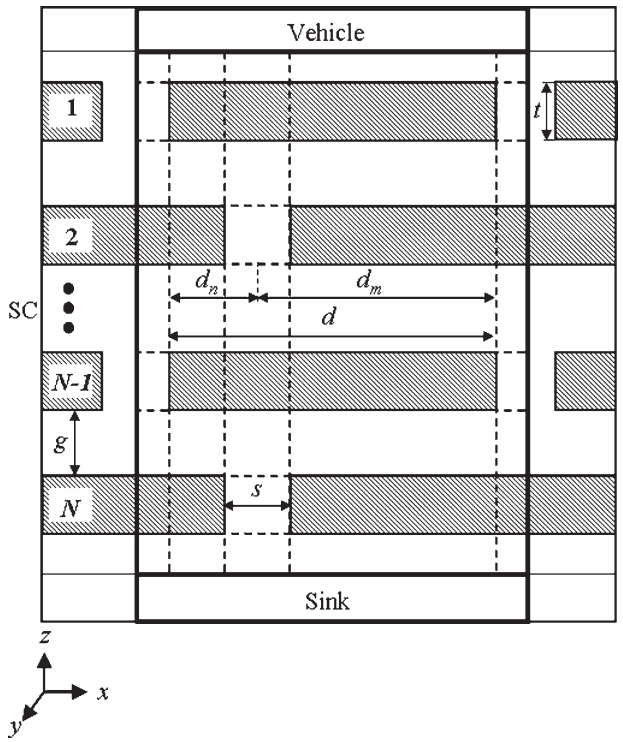

Figure 2. Schematic diagram of the "bricks-and-mortar" model of human stratum corneum (SC).

Corneocyte width (d), corneocyte thickness (t), number of corneocyte layers (N), the vertical gap between corneocytes (g), the lateral spacing between corneocytes (s), and the offset ratio ($w = d_m/d_n$).

From the computer simulation, the various components of the mass-balance equation can be obtained. As an overestimation, the amount of solute delivered across the SC to the epidermis and dermis can be considered as bioavailable. The bioavailability of a topically applied solute, is, thus, estimated as

$$F = \frac{M_d}{AC_0h} = \frac{\int_0^t q_d dt}{C_0h} \tag{3}$$

Model evaluation

The accuracy of the model prediction is evaluated by Akaike's information criterion (*AIC*). The *AIC* is calculated as follows

$$AIC = 2k + n(\ln(2\pi \times MSE) + 1) \tag{4}$$

where k is the number of fitting parameters, n is the sample number, *MSE* is the mean squared error and is calculated by the following equation

$$MSE = \frac{\sum_{i=1}^{n} (Y_i^{obs} - Y_i^{pre})^2}{n} \tag{5}$$

where Y_i^{obs} is the observed value, Y_i^{pre} is the predicted value.

Results and Discussion

Prediction of tape striping data of 4-cyanophenol

The *in vivo* transdermal permeation process has described by Stinchcomb et al.[29] The vehicle is simulated as an infinite source with a constant concentration of 4-cyanophenol at saturation of 0.11 mol/L. The initial concentration of 4-cyanophenol was 0.31 mol/L which is well above the saturation point. The vehicle thickness is 0.7 mm and the experimental duration did not exceed 15 min. The 4-cyanophenol concentration during the experiment period did not drop below the saturation concentration of 0.11 mol/L. As a result, it is reasonable to consider the vehicle as an infinite source. With the experiment, an aqueous solution was applied to the skin and the water content of the *SC* was likely to increase and reach saturation fairly quickly under the occlusive experimental condition. In our simulation, we assume the hydration process is much faster than the transdermal permeation of 4-cyanophenol. Thus, as an overestimation, the water content in the SC was set to 55% across the SC depth in the simulation. The diffusion and partition properties of 4-cyanophenol in human *SC* lipid and corneocytes are calculated using the equations proposed in Part 1 of this article.[42] The calculated partition and diffusion properties used for predicting 4-cyanophenol permeation *in vivo* are summarized in Table 1. Figure 3a shows the predicted concentration profiles of 4-cyanophenol along the depth of the SC as a function of time, in comparison with the original experimental data. The model prediction agreed reasonably well with the experimental data. It appears there are some deviations in the prediction at a longer time (15 min) as is discussed later.

Stinchcomb et al.[29] also tried to model the data using the simple diffusion equation, assuming the SC as a homogeneous media, but did not obtain satisfactory agreement. The simple diffusion model of Stinchcomb et al.[29] gave an *AIC* value of -20.71, whereas the current model gives a much improved *AIC* value of -33.57. With the simple diffusion model, Stinchcomb et al.[29] showed that the concentration at the top layer of the SC did not change with time. Recently, Herkenne et al.[38] used a similar approach for dermatopharmacokinetic prediction of topical drug bioavailability *in vivo,* and also predicted a fixed concentration of ibuprofen at the top surface of the SC. This is unlikely because it takes time for the solute concentration to buildup. Indeed, the available tape-striping data[28,29] showed a gradual buildup of topically applied solute along the depth of the SC including the top layer at the early stage after the topical exposure.

The prediction of our model can be further improved by allowing the parameters of the model to be optimized. There are four mechanism based physical parameters including the

Table 1. Theoretically Calculated Diffusion and Partition Properties of 4-Cyanophenol in Human SC Lipid and Corneocytes

Parameters	Values
Diffusivity in water (36°C)	9.12×10^{-10} m^2/s
Octanol-water partition coefficient	39.8
Diffusivity in the SC lipid	3.59×10^{-11} m^2/s
SC lipid-water partition coefficient	13.18
Diffusivity in SC corneocytes	2.92×10^{-15} m^2/s
SC corneocyte-water partition coefficient	6.23

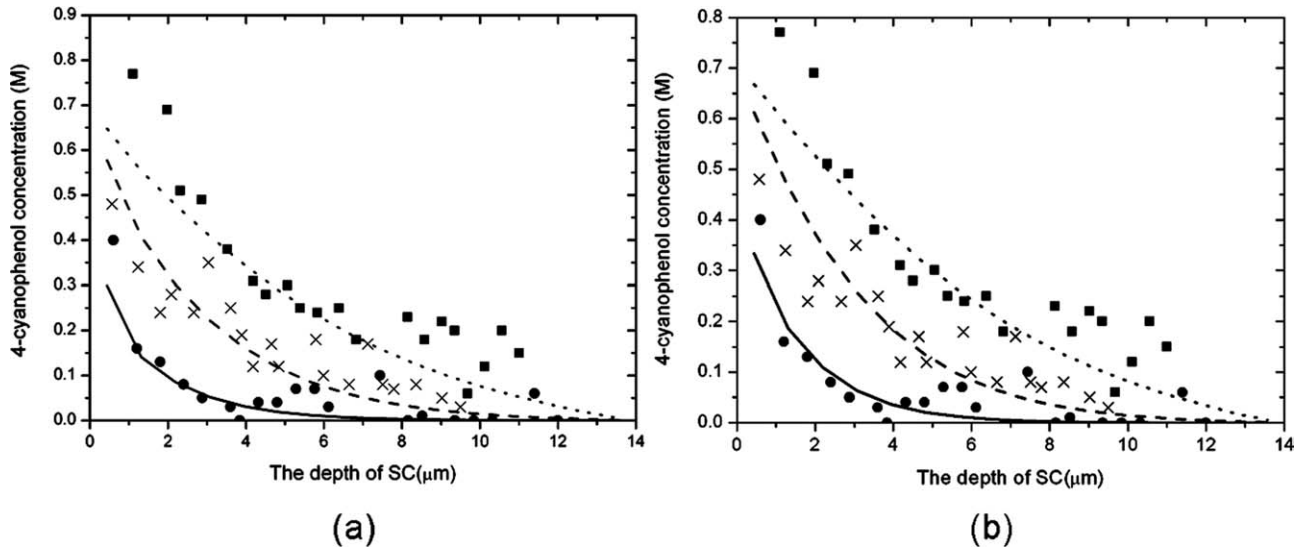

Figure 3. Model prediction (lines) compared with *in vivo* tape-striping data of 4-cyanophenol permeation into the SC of the forearm of a health volunteer after exposure times of 1 min (●), 5 min (×), and 15 min (■) to a saturated aqueous solution.

(a) Model prediction with theoretical values of partition and diffusion properties, and (b) model prediction with optimized values of partition and diffusion properties. The *in vivo* experimental data is from Stinchcomb et al.[29]

partition coefficient between lipid and water (P_{mw}), partition coefficient between corneocytes and water (P_{bw}), diffusion coefficient in the lipid phase (D_m), and diffusion coefficient in the corneocytes phase (D_b). When the four parameters are allowed to ''float'', the prediction is further improved and the corresponding *AIC* value is further reduced to −35.66. The optimized values of the four parameters are $P_{mw} = 11.4$, $P_{bw} = 6.5$, $D_m = 4.0 \times 10^{-11}$ m^2/s, and $D_b = 2.0 \times 10^{-15}$ m^2/s. The optimized parameters compare closely to the theoretically-derived values of $P_{mw} = 13.2$, $P_{bw} = 6.2$, $D_m = 3.6 \times 10^{-11}$ m^2/s, and $D_b = 2.9 \times 10^{-15}$ m^2/s. Figure 3b shows the simulation results compared with the experimental data when optimized values of the four parameters are used. Although the prediction is slightly improved by optimizing the model parameters, there are still some deviations at 15 min. There reasons are not very certain. The current model assumed the boundary condition beneath stratum corneum as an infinite sink. The underlying assumption is that the clearance of solute in this relatively high-water content environment is sufficiently fast. It is possible there could be some buildup of solute concentration in the epidermis at longer time, pushing up the solute concentration in the lower part of the stratum corneum. This partially explains why the current model underpredicted the solute concentration at longer time in the lower region. Still more experimental and modeling studies are needed to resolve this uncertainty.

Prediction of confocal Raman spectrometry data of transretinol

The confocal raman spectrometry *in vivo* measurement of Pudney et al.[35,36] involves the application of 0.07 mL 70:30 (v/v) ethanol/propylene glycol solution and myritol 318 solution, both containing 0.3% (wt) of transretinol to an area of 4×4 cm^2 of the volar forearm of two male volunteers of 30 and 40 years of age. Here, the vehicle is simulated as a finite volume. With the ethanol/propylene glycol solution, ethanol is expected to evaporate rapidly within a few minutes of application, leading to an increased transretinol concentration of 1% in the remaining propylene glycol. In the simulation, the evaporation of ethanol is not directly modeled. Instead, it is assumed that ethanol evaporation completed in a time scale that is negligibly short compared to the penetration of transretinol. The average thickness of the remaining propylene glycol is reduced to 13 μm. For Myritol 318 oil, the initial thickness of the vehicle is 43.75 μm, and the initial concentration is 0.3%. During the experiment the arm was repeatedly moved away from the instrument to prevent occlusions effect. Some of the applied solution was left on the window which was cleaned before the arm was replaced onto the instrument. The loss of the vehicle material during the experiment is simulated by reducing the film thickness. The partition coefficient of retinol between propylene glycol and water is set to 1,300, and that between Myritol oil and water is set to 4,800, both estimated by considering the equilibrium of transretinol between the vehicle and the lipid at the top layer of the SC after 30 min of application. The diffusion coefficient of transretinol in the vehicle is estimated using the Einstein-Stokes equation.

Unlike the tape-striping study which involved topical application of saturated aqueous solution of 4-cyanophenol under occlusive condition, the experimental condition of confocal Raman study is unlikely to cause significant changes of skin hydration levels. Thus, in the simulation, the water content is set to the natural hydration level, varying between 25 and 55% from the top to the bottom of the SC, the same range quantified in the experiment.[36] Other ''bricks-and mortar'' structure parameters and properties of the SC are kept to be the same. The calculated partition and diffusion properties used for predicting transretinol permeation *in vivo* are summarized in Table 2. Transdermal

Table 2. Theoretically Calculated Diffusion and Partition Properties of Transretinol in Human SC Lipid and Corneocytes

Parameters	Values
Diffusivity in water (36°C)	6.81×10^{-10} m^2/s
Octanol-water partition coefficient	478630
Diffusivity in the SC lipid	1.47×10^{-12} m^2/s
SC lipid-water partition coefficient	9462
Diffusivity in SC corneocytes	$1.6 \times 10^{-17} \sim 1.0 \times 10^{-15}$ m^2/s*
SC corneocyte-water partition coefficient	71.14 ~ 71.61

*Variation due to the change in the water content.

permeation of transretinol is predicted for both vehicles of Myritol 318 oil and 70:30 (v/v) ethanol/propylene glycol solutions. Figure 4 shows the predicted retinol concentration profiles in the SC after 30 min of application of the two vehicles, in comparison with the experimental data. The agreement is very good. Here, we observe that the ethanol/propylene glycol vehicle resulted in an order of magnitude increase in the transretinol concentration buildup in the SC compared to Myritol 318. After ethanol evaporation, the transretinol concentration in the ethanol/propylene glycol vehicle would be increased three times higher than that in the Myritol 318 oil.. The computer simulation undoubtedly illustrates that the lower partition coefficient of retinol between propylene glycol vehicle and water favored the absorption of retinol into the lipid phase of the SC, and resulted in an additional increase of more than a three-fold increase in the concentration buildup of retinol in the SC. In fact, the vehicle-water partition coefficient of propylene glycol is about 1/3 of that of Myritol 318 oil, indicating good scaling between the vehicle-water partition coefficient and the initial concentration and percutaneous absorption.

Propylene glycol is a good permeation enhancer. Pudney et al.[36] showed that there was a significant amount of propylene glycol penetrated into the SC. It is shown in Figure 5

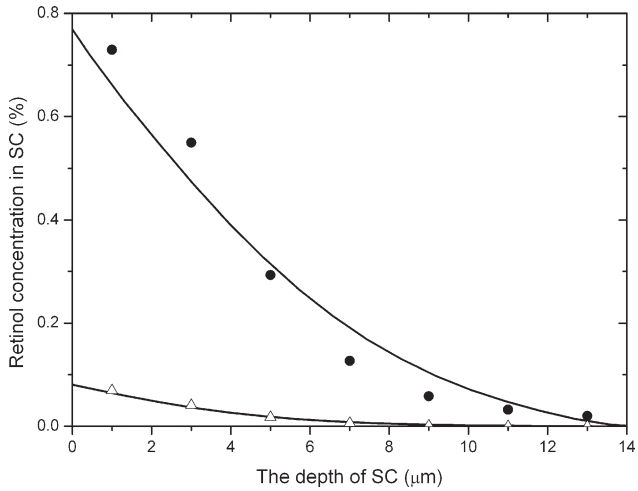

Figure 4. Model prediction (lines) of transretinol distribution after exposure time of 30 min of topical application of 70:30 (v/v) ethanol/propylene glycol (●) and Myritol 318 oil (△), both containing 0.3% transretinol, to the forearm of a health volunteer.

The *in vivo* experimental data is obtained using confocal Raman spectrometry by Pudney et al.[36]

that better prediction of transretinol absorption by the SC can be obtained when the diffusion coefficient of transretinol in the lipid matrix is increased from the theoretical value of 1.47×10^{-12} m^2/s to 3.19×10^{-12} m^2/s, an increase of more than two-fold. The increased diffusion coefficient may be contributed to two reasons. First, the permeation of propylene glycol into the SC is likely to change the permeation property of the SC. Second, in addition to the diffusive permeation, the penetration of propylene glycol into the SC will bring additional dissolved transretinol into the skin. Here we

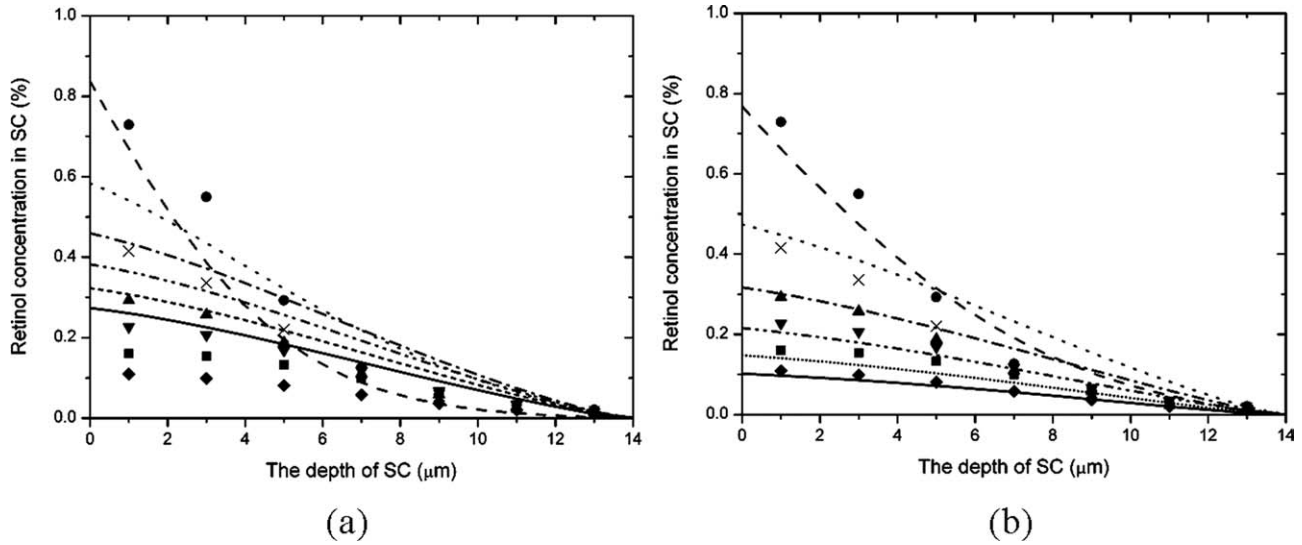

Figure 5. Concentration profiles of transretinol in the SC following the administration of 70:30 (v/v) ethanol/propylene glycol containing 0.3% transretinol to the forearm of a health volunteer.

Model prediction (lines) compared with confocal Raman spectrometry data. (a) Direct prediction with theoretical value Dm = 1.47e–12 m^2/s, and (b) prediction with optimized value Dm = 3.19e–12 m^2/s. The *in vivo* experimental data is from Pudney et al.[36]

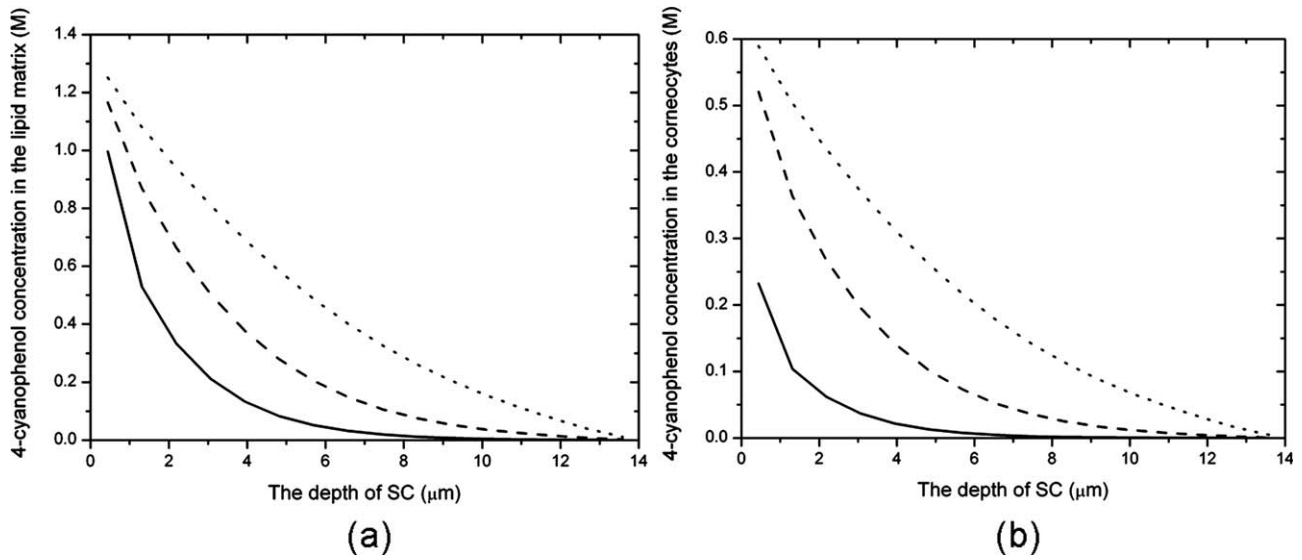

Figure 6. Predicted concentration profiles of 4-cyanophenol in the lipid matrix (a) and corneocytes, and (b) of the SC at 1 min ———, 5 min --- and 15 min ..... of exposure time of topically administered saturated aqueous solution as described by Stinchcomb et al.[29]

also observe that when the theoretical value of diffusion is used, the model prediction is reasonably good at shorter times, but deviated at longer times with significant overprediction. When the diffusion coefficient is allowed to float to the optimal value, the prediction is much improved for longer times, but there are some mismatches at shorter times. This is opposite to the prediction of the tape striping data. There are significant differences in the experimental conditions between the tape strip and Raman confocal experiments. With the Raman confocal experiment, the stratum corneum top layer as not fully hydrated as the lower part. Strictly speaking, the transdermal absorption of transretinol is not only by diffusion, but also by infiltration of the vehicle, as shown by the original experimental studies.[36] As the vehicle penetrates it is probably changes the local skin structure, and, therefore, the diffusion coefficient is likely to change. In addition, the penetration of the vehicle will also bring in some solute. The current model did not simulate this vehicle infiltration explicitly, and the use of constant effective diffusion coefficient to represent vehicle infiltration did not take into account such nonlinear effect is likely to cause errors. Clearly, more studies are needed to improve the prediction of transdermal permeation.

Prediction of dermatopharmacokinetic parameters

From the point of view of percutaneous absorption and bioavailability, much of the concern is to design the formulation and application regimes to deliver active molecules to targeted receptors at therapeutically relevant rate and concentration, whether it is a drug molecule or a cosmetics active molecule.[2,26,38] Predicting the relevant amount of solute permeated across the SC to the dermis and viable epidermis is also required for safety assurance of skin sensitizing chemicals. With the computer simulation, many such dermatopharmacokinetic parameters of transdermal permeation and bioavailability can be obtained. First, the computer model directly predicts how many active molecules are absorbed and stored in the heterogeneous structures of the SC (Figure 6). For instance, 4-cyanophenol is a moderately hydrophobic molecule with $K_{ow} = 40$. It is widely believed that corneocytes are impermeable to hydrophobic solutes, and the tortuous lipids pathway is the main pathway for transdermal permeation. However, the computer simulation indicates that this is not necessarily the case. The concentration of 4-cyanophenol in the corneocytes is predicted to have reached half of that in the lipid matrix. Corneocytes contributes to more than 80% of mass of the SC. It follows that the actual amount of 4-cyanophenol stored in the corneocytes is more than twice of that stored in the lipid matrix. Thus, for moderately hydrophobic solutes like 4-cyanophenol, corneocytes phase, has an important effect on percutaneous absorption. Only for highly hydrophobic solutes, their partition into the corneocytes can be ignored. For transretinol, the concentration of transretinol in the corneocytes is orders of magnitude lower than that in the lipid matrix, and the contribution of transcellular pathway across the corneocytes is negligibly small.

The aforementioned prediction that a significant amount of moderately hydrophobic solute like 4-cyanophenol partitions into the corneocytes and contributes significantly to the percutaneous absorption is irrefutable. Published tape-stripping data showed that the overall concentration of 4-cyanophenol in the top layers of the SC reached as high as about 0.8 mol/kg of the SC.[28,29] If the partition and storage of 4-cyanophenol into corneocytes is ignored, the maximum concentration of 4-cyanophenol that the lipid matrix can reach at equilibrium, with the saturated concentration of 4-cyanophenol in the aqueous phase is estimated to be mol/kg lipid. This contributes to an overall 4-cyanophenol concentration of less than 0.3 mol/kg of the wet tissue of the SC, which is well below the measured data of ca 0.8 mol/kg.[29,38] Clearly, for moderately hydrophobic solutes like 4-cyanophenol, partition to the corneocytes and absorption by this phase cannot be ignored. This can be also supported by our early study on

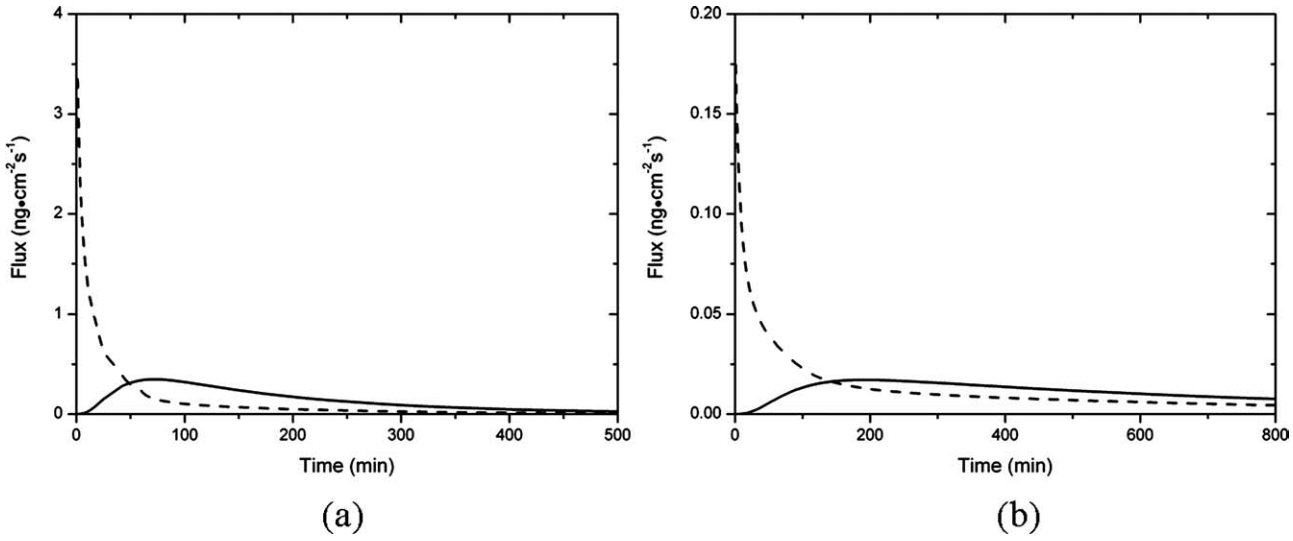

Figure 7. Predicted rate of transretinol absorption by the skin (dashed line), and rate of transretinol delivered to the epidermis and dermis from the SC (solid line) following the topical exposure to (a) 70:30 (v/v) ethanol/propylene glycol solution, and (b) the Myritol 318 oil, both containing 0.3% transretinol as described by Pudney et al.[36]

modeling skin permeability (Part 1), where it is shown that for many moderately hydrophobic solutes, transdermal permeation pathway still contribute to up to 25% of the overall skin permeability. For 4-cyanophenol, it is predicted that the contribution from the transcellular pathway constitute about 10% of its overall skin permeability.

Figure 7 shows the predicted rates of transretinol absorption by the skin and that delivered to the epidermis and dermis following the topical application of two different solutions of 70:30 (v/v) ethanol/propylene glycol and Myritol 318 oil, both containing 0.3% transretinol. The rate of transretinol absorption by the skin decreases with time. The rate of transretinol delivery to the epidermis and dermis across the SC increases with time initially and reaches a maximum. The rate of transretinol delivered to the epidermis and dermis exceeded that absorbed by the skin at later stage. This corresponds to a reduction of transretinol concentration in the SC. With the 70:30 (v/v) ethanol/propylene glycol solutions, it is predicted that there is about 20-fold increase in the rate of percutaneous absorption of transretinol compared to that of Myritol 318 oil. The rate of transretinol delivered to the epidermis and dermis by ethanol/propylene glycol is also about 20-fold higher than that by Myritol 318 oil. The 20-fold increase can be resolved into three parts: 3.3-fold increase in the initial concentration of transretinal in the ethanol-propylene solution following the rapid evaporation of ethanol, three-fold increase of transretinol partition into the skin lipid due to the lower vehicle-water partition coefficient of propylene glycol, and two-fold increase enhanced by the permeation of propylene glycol into the SC.

Retinol is a skin care active molecule widely used for acne treatment and skin repair. Regular application of retinol containing creams will eventually make skin soft and smooth. However, for retinol to be functionally effective, it is necessary for it to penetrate through the SC and reach the skin receptors of retinoic acid so that the reproduction of cells in the epidermis and dermis region can be enhanced. Figure 8 shows that throughout the topical application transretinol bioavailability is relatively low. With Myritol 318 oil, the amount of transretinol delivered to the epidermis and dermis did not exceed 7% after more than 10 h of administration. The amount of transretinol delivered by ethanol/propylene glycol solution is much increased: about 34% of the administered transretinol delivered to the epidermis and dermis region after about 10 h of application.

Conclusions

Although significant progresses have been made recently in monitoring transdermal permeation and absorption of

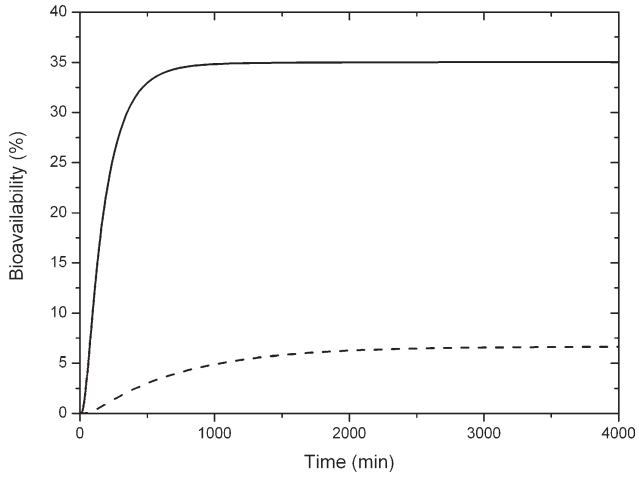

Figure 8. Predicted bioavailability of transretinol in the epidermis and dermis across the SC following the topical exposure to 70:30 (v/v) ethanol/propylene glycol solution (solid line), and Myritol 318 oil (broken line), both containing 0.3% transretinol as described by Pudney et al.[36]

topically administered solute *in vivo*, the methods are still limited to solute distribution in the top layer of the SC of less than 20 μm. Percutaneous absorption and bioavailability of topically administered active molecules in the deeper layer of epidermis and dermis is still difficult to obtain. Most modeling studies in the area tend to use simple diffusion models to derive dermal parameters such as permeability by fitting to the same experimental data to be modeled. Here, we apply our mechanistic model to predict transdermal permeation and bioavailability *in vivo*. The diffusion and partition properties of the SC, and the vehicle are estimated theoretically from the fundamental physical and chemical properties of the solute. Two sets of *in vivo* data have been modeled: the tape-striping data of 4-cyannophenol from Stinchcomb et al.[29] and the confocal Raman spectrometry data of transretinol from Pudney et al.[36] The model prediction agreed well with the experimental data.

With the model prediction, many dermatopharmacokinetic parameters of percutaneous absorption and bioavailability can be further derived. These include the distribution of solute in lipid matrix and corneocytes, and the effects of vehicle formulation and topical application condition on transdermal permeation. In particular, the delivery of solute deeper into epidermis and dermis region has been quantified. The mechanism-based model is demonstrated to be capable of not only predicting *in vivo* data of transdermal permeation, but also providing much insight into the dermatopharmacokinetics of percutaneous absorption and bioavailability in the epidermis and dermis region.

Acknowledgments

This research is jointly supported by Unilever R&D Colworth and China Agricultural University (Contract No. 2008005). We also acknowledge the help of River Diagnostics in obtaining the previously published Raman data.

Literature Cited

1. Langer RS. Designing materials for biology and medicine. *Nature*. 2004;428:487–491.
2. Elsayed MMA, Abdallaha OY, Naggara VF, Khalafallah NM. Lipid vesicles for skin delivery of drugs: Reviewing three decades of research. *Int J Pharm*. 2007;332:1–16.
3. Harada K, Murakami T, Yata N, Yamamoto S. Role of intercellular lipids in straum corneum in the percutaneous permeation of drugs. *J Invest Dermatol*. 1992;99:278–282.
4. Jung S, Otberg N, Thiede G, Richter H, Sterry W, Panzner S, Lademann J. Innovative liposomes as a transfollicular drug delivery system: penetration into porcine hair follicles. *J Invest Dermatol*. 2006;126:1728–1732.
5. Abramovits W, Gonzalez-Serva A. Sebum, cosmetics, and skin care. *Dermatol Clin*. 2000;18:617–620.
6. Wu C, Chiu H. Rapid method for determining dermal exposures to pesticides by use of tape stripping and FTIR spectroscopy: a pilot study. *J Occup Environ Hyg*. 2007;4:952–958.
7. Surber C, Wilhelm KP, Maibach HI, Hall LL, Guy RH. Partitioning of chemicals into human stratum corneum: implications for risk assessment following dermal exposure. *Fund Appl Toxicol*. 1990; 15:99–107.
8. Mclean WH, Hull PR. Breach delivery: increased solute uptake points to a defective skin barrier in atopic dermatitis. *J Invest Dermatol*. 2007;127:8–10.
9. Blank IH. Transport across the stratum corneum. *Toxicol Appl Pharmacol Suppl*. 1969;3:23–29.
10. Scheuplein RJ. Percutaneous absorption after twenty-five years: or "old wine in new wineskins". *J Invest Dermatol*. 1976;61:31–38.
11. Abraham MH, Chadha HS, Mitchell RC. The factors that influence skin penetration of solutes. *J Pharm Pharmacol*. 1995;47:8–16.
12. Al-Amoudi A, Dubochet J, Norlen L. Nanostructure of epidermal extracellular space as observed by cryo-electron microscopy of vitreous sections of human skin. *J Invest Dermatol*. 2005;124:764–777.
13. Anderson BD, Raykar PV. Solute structure-permeability relationships in human stratum corneum. *J Invest Dermatol*. 1989;93:280–286.
14. Bouwstra JA, Dubbelaar FER, Gooris GS, Weerheim AM, Ponec M. The role of ceramide composition in the lipid organization of the skin barrier. *Biochimica Biophysica Acta*. 1999;1419:127–136.
15. Elias PM. Lipids and the epidermal permeability barrier. *Arch Derm Res*. 1981;270:95–117.
16. Kasting GB, Barai ND, Wang TF, Nitsche JM. Mobility of water in human stratum corneum. *J Pharm Sci*. 2003;92:2326–2340.
17. Michaels AS, Chandrasekaran SK, Shaw JE. Drug permeation through human skin-theory and in-vitro experimental measurement. *AIChE J*. 1975;21:985–996.
18. Mitragotri S. A theoretical analysis of permeation of small hydrophobic solutes across the stratum corneum based on scaled particle theory. *J Pharm Sci*. 2002;91:744–752.
19. Norlen L, Al-Amoudi A, Dubochet J. A cryotransmission electron microscopy study of skin barrier formation. *J Invest Dermatol*. 2003;120:555–560.
20. Potts RO, Guy RH. Predicting skin permeability. *Pharm Res*. 1992;9:663–669.
21. Wang TF, Kasting GB, Nitsche JM. A multiphase microscopic diffusion model for stratum corneum permeability. I. Formulation, solution, and illustrative results for representative compounds. *J Pharm Sci*. 2006;95:620–648.
22. Wang TF, Kasting GB, Nitsche JM. A multiphase microscopic diffusion model for SC permeability. II. estimation of physicochemical parameters and application to a large permeability database. *J Pharm Sci*. 2007;96:3024–3051.
23. Wertz PW, van der Bergh B. The physical, chemical and functional properties of lipids in the skin and other biological barriers. *Chem Phys Lipids*. 1998;91:85–96.
24. Wilschut A, Tenberge WF, Robinson PJ, T.E. M. Estimating skin permeation - The validation of 5 mathematical skin permeation models. *Chemosphere*. 1995;30:1275–1296.
25. Cross SE, Magnusson BM, Winckle G, Anissimov Y, Roberts MA. Determination of the effect of lipophilicity on the *in vitro* permeability and tissue reservoir characteristics of topically applied solutes in human skin layers. *J Invest Dermatol*. 2003;120:759–764.
26. Kogan A, Garti N. Microemulsions as transdermal drug delivery vehicles. *Adv Colloid Interface Sci*. 2006;123:369–385.
27. Herkenne C, Naik A, Kalia YN, Hadgraft J, Guy RH. Pig ear skin ex vivo as a model for in vivo dermatopharmacokinetic studies in man. *Pharm Res*. 2006;23:1850–1856.
28. Reddy MB, Stinchcomb AL, Guy RH, Bunge AL. Determining dermal absorption parameters in vivo from tape strip data. *Pharm Res*. 2002;19:292–298.
29. Stinchcomb AL, Pirot F, Touraille GD, Bunge AL, Guy RH. Chemical uptake into human stratum corneum in vivo from volatile and non-volatile solvents. *Pharm Res*. 1999;16:1288–1293.
30. Rajadhyaksha M, Gonzalez S, Zavislan JM, Anderson RR, Webb RH. In vivo confocal scanning laser microscopy of human skin II: Advances in instrumentation and comparison with histology. *J Invest Dermatol*. 1999;113:293–303.
31. Caspers PJ, Lucassen GW, Puppels GJ. Combined in vivo confocal Raman spectroscopy and confocal microscopy of human skin. *Biophysical J*. 2003;85:572–580.
32. Caspers PJ, Lucassen GW, Bruining HA, Puppels GJ. Automated depth-scanning confocal Raman microspectrometer for rapid in vivo determination of water concentration profiles in human skin. *J Raman Spectrosc*. 2000;31:813–818.
33. Caspers PJ, Lucassen GW, Wolthuis R, Bruining HA, Puppels GJ. In vitro and in vivo raman spectroscopy of human skin. *Biospectroscopy*. 1998;4:S31–S39.
34. Caspers PJ, Lucassen GW, Carter EA, Bruining A, Puppels GJ. In vivo confocal Raman microspectroscopy of the skin: noninvasive determination of molecular concentration profiles. *J Invest Dermatol*. 2001;116:434–442.

35. Mélot M, Pudney PDA, Williamson AM, Caspers PJ, Van Der Pol A, Puppels GJ. Studying the effectiveness of penetration enhancers to deliver retinol through the stratum cornea by in-vivo confocal Raman spectroscopy. *J Control Rel*. 2009;138:32–39.
36. Pudney PDA, Mélot M, Caspers PJ, Van Der Pol A, Puppels GJ. An in vivo confocal raman study of the delivery of trans-retinol to the skin. *Appl Spectrosc*. 2007;61:804–811.
37. Xiao C, Moore DJ, Rerek ME, Flach CR, Mendelsohn R. Feasibility of tracking phospholipid permeation into skin using infrared and Raman microscopic imaging. *J Invest Dermatol*. 2005;124:622–632.
38. Herkenne C, Naik A, Kalia YN, Hadgraft J, Guy RH. Dermatopharmacokinetic prediction of topical drug bioavailability in vivo. *J Invest Dermatol*. 2007;127:887–894.
39. McCarley KD, Bunge AL. Physiologically relevant two-compartment pharmacokinetic models for skin. *J Pharm Sci*. 2000;89:1212–1235.
40. Reddy MB, McCarley KD, Bunge AL. Physiologically relevant one-compartment pharmacokinetic models for skin. 2. Comparison of models when combined with a systemic pharmacokinetic model. *J Pharm Sci*. 1998;87:483–490.
41. Chen LJ, Lian GP, Han LJ. Use of "bricks and mortar" model to predict transdermal permeation: model development and initial validation. *Ind Eng Chem Res*. 2008;47:6465–6472.
42. Chen LJ, Lian GP, Han LJ. Modeling transdermal permeation. Part I. Predicting skin permeability of both hydrophobic and hydrophilic solutes. *AIChE J*. 2010:56:1136–1146.
43. Pudney PDA, Hancewicz TM, Cunningham DG, Brown MC. Quantifying the microstructures of soft solid materials by confocal Raman spectroscopy. *Vib Spectrosc*. 2004;34:123–135.

Manuscript received Feb. 11, 2009, revision received Sept. 18, 2009, and final revision received Dec. 1, 2009.